

WRF simulations across scales (WRFSCALE)

Hans-Stefan Bauer, Thomas Schwitalla, Oliver Branch, Rohith Thundathil and Volker Wulfmeyer
University of Hohenheim, Institute of Physics and Meteorology (IPM), Stuttgart, Germany



1) Scientific Background and Goals

Numerical models are excellent tools to improve our understanding of atmospheric processes across scales, since they provide the full 4D representation of the atmosphere and produce a consistent state with respect to the prognostic and diagnostic variables.

For a realistic representation of mesoscale processes, especially in terms of the spatial and temporal distribution of precipitation, a grid resolution of less than 3 km is necessary. Further improvements are expected if a chain of grid refinements is performed down to the turbulence scale (100 m and below), as further details of land-surface atmosphere (LSA) interaction are resolved (e.g. Bauer et al., 2020).

2) Investigation of the boundary layer evolution

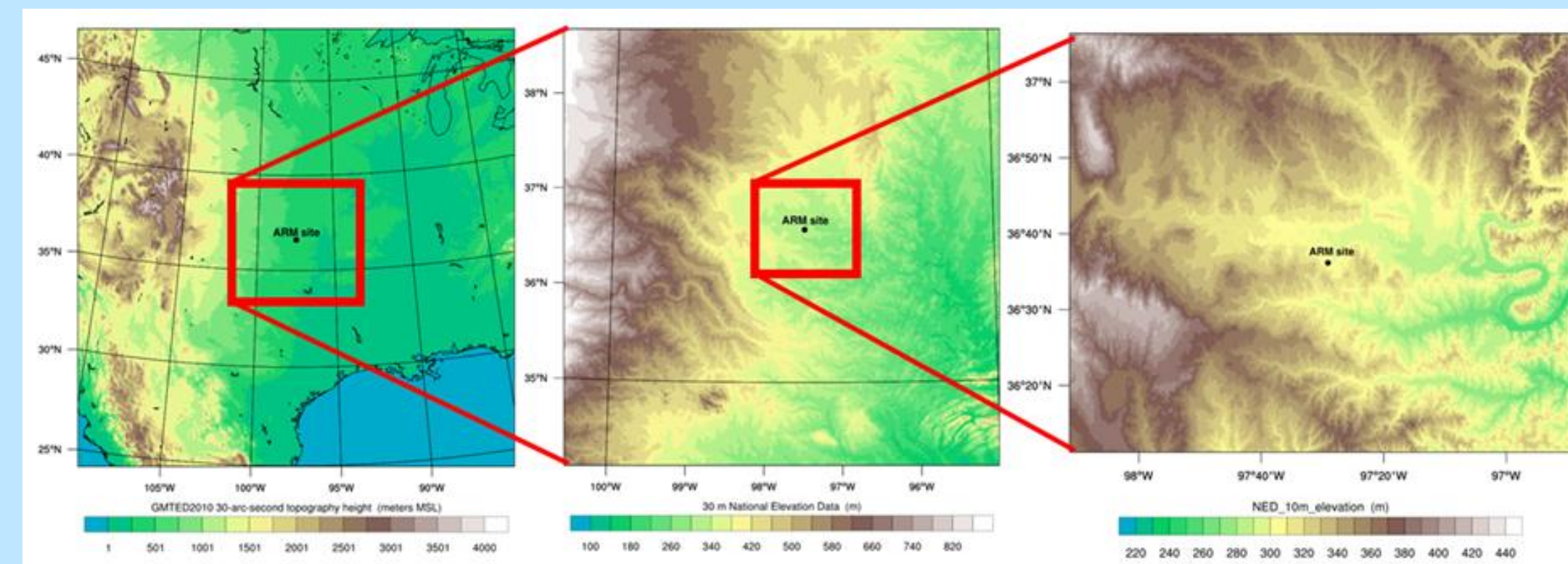


Figure 1: Domain configuration of the first LAFE simulation. From left to right the domains with 2500 m, 500 m and 100 m resolution.

- WRF version 4.1.5
- Three domains with 2500 m, 500 m, and 100 m resolution and 100 vertical levels up to 50 hPa.
- High-resolution topography, land cover and soil initialization
- Sophisticated physics and no turbulence scheme in the inner two domains.
- Output every five minutes

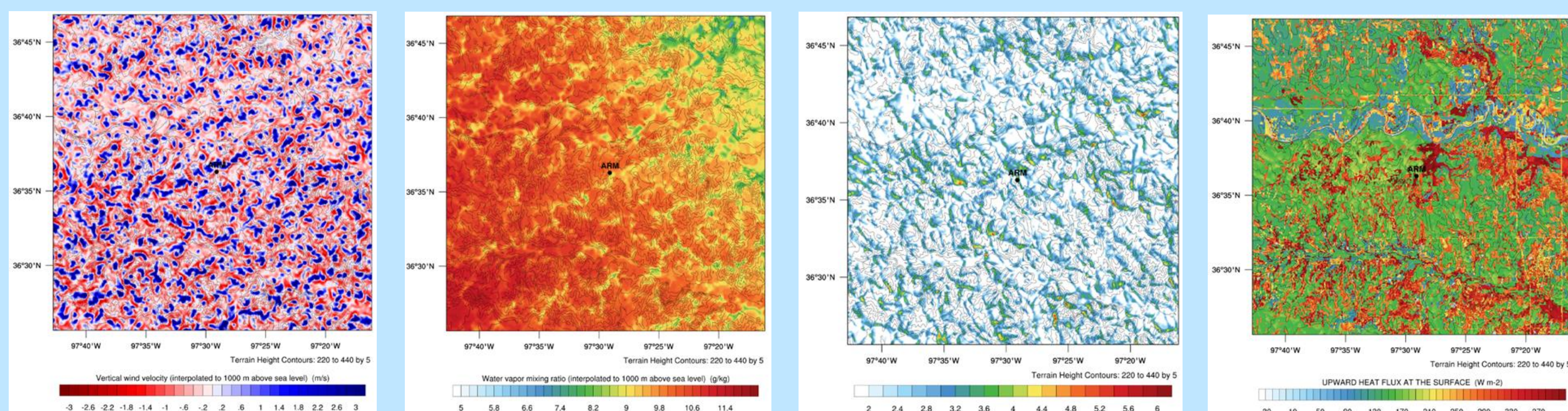


Figure 2: Representation of the convective boundary layer zoomed into a small region around the ARM SGP site at 2 p.m. on 23 August 2017. From left to right: Vertical velocity (m/s) and water vapor mixing ratio (g/kg) 1000 m above sea level, 10 m wind velocity (m/s) and surface sensible heat flux (W/m²).

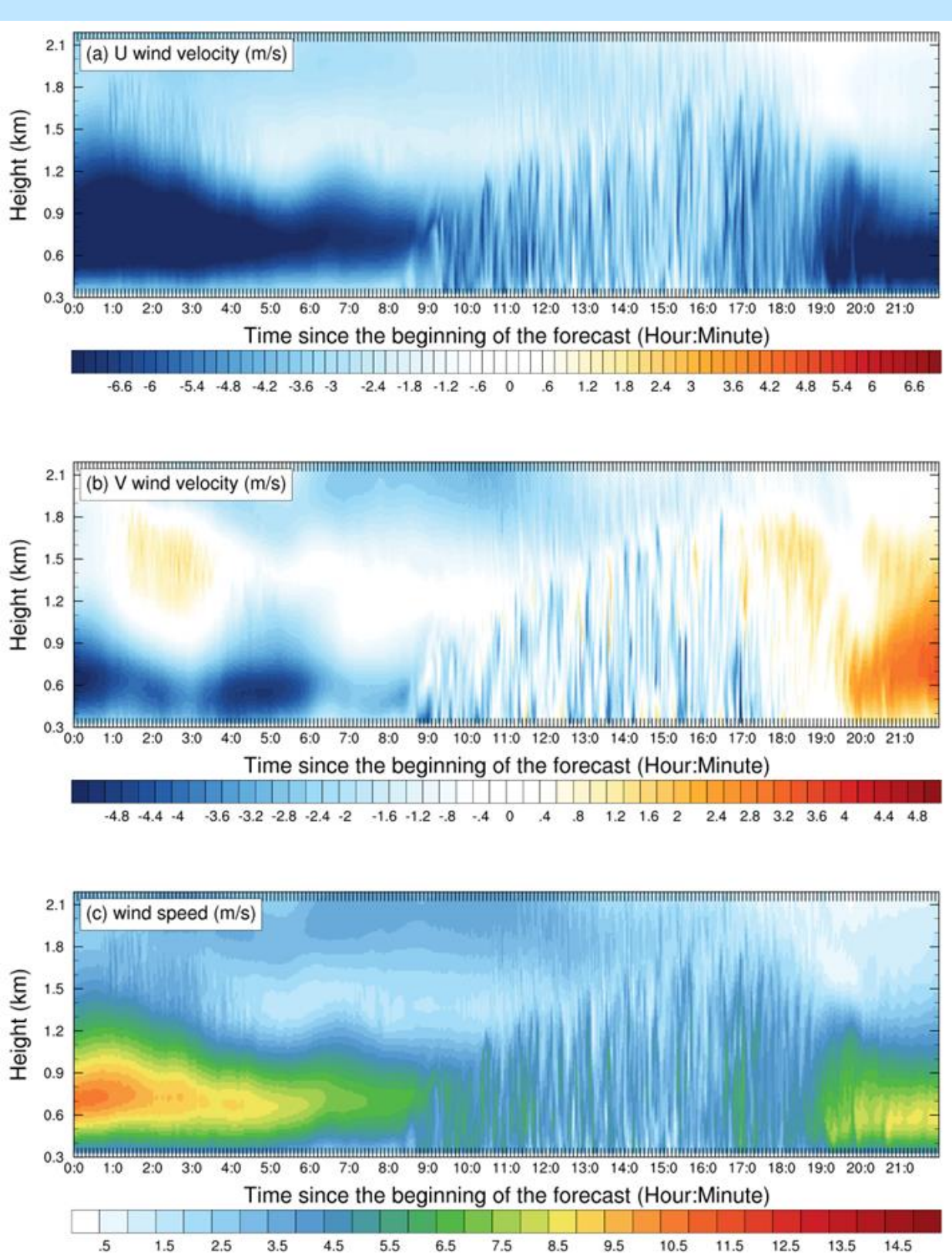


Figure 3: Time-height cross sections of the west-east (top) and the south-north (middle) component of the wind velocity (m/s). The bottom panel shows the total wind velocity. The X-Axis marks the time in hours since the beginning of the forecast (00 = 06 UTC or 01 local time in Oklahoma).

- Horizontal, vertical and temporal evolution of the turbulent boundary layer is well represented.
- It is our first simulation that covers both the morning and evening transitions between the nighttime and daytime boundary layer.
- Additional time series output at selected grid points allow a detailed comparison of the model results with lidar and other data collected during the Land Atmosphere Feedback Experiment (LAFE).
- Such comparisons are ongoing research and aim to improve the process understanding and their representation in the model.

3) Seasonal land surface modification simulations over the United Arab Emirates (UAE)

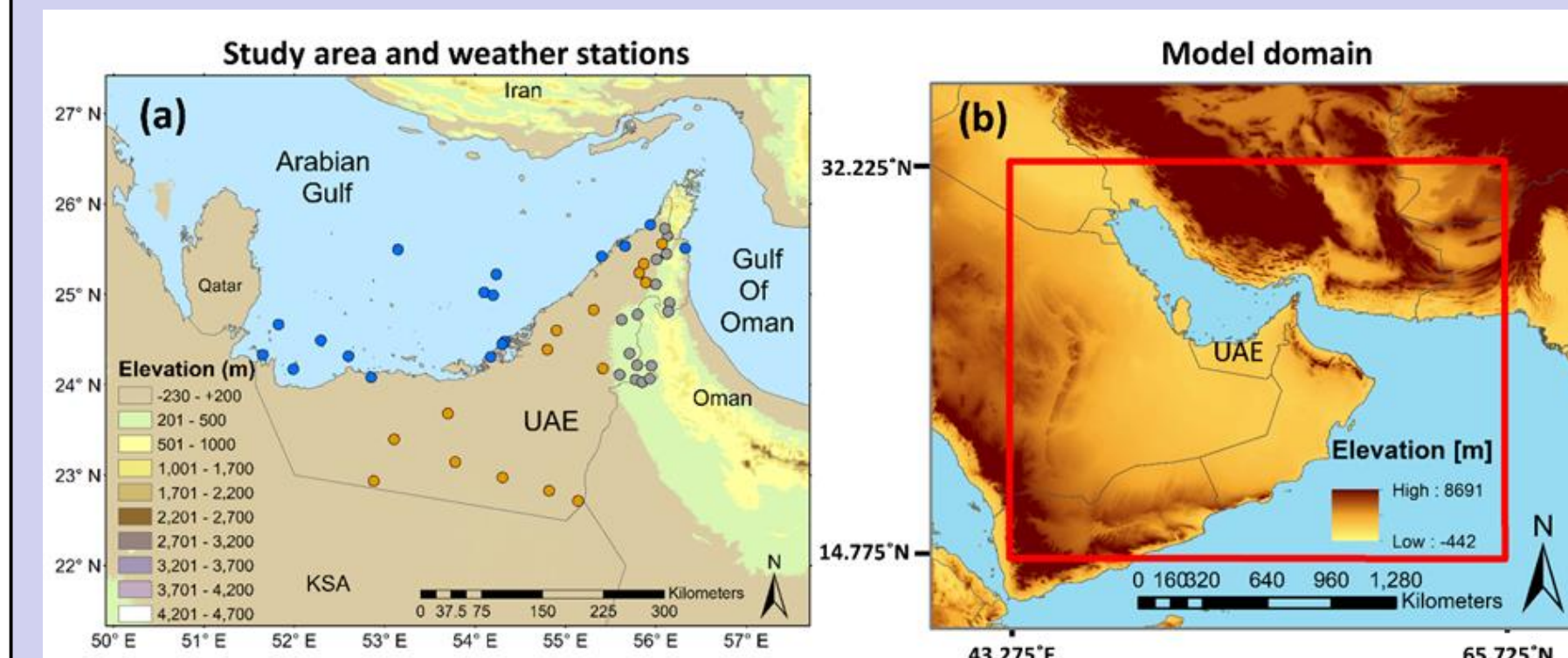


Figure 4: The study area (left) showing the UAE with the 48 weather stations on which comparisons were made. These are split into three groups – grey dots, mountain – orange dots, desert – blue dots, marine.

- WRF was setup with 0.025° horizontal resolution and a domain size of 900 x 700 grid cells (Fig. 4b).
- Daily simulations were performed in forecast mode for the period January 01 to November 30, 2015 and compared with station observations.

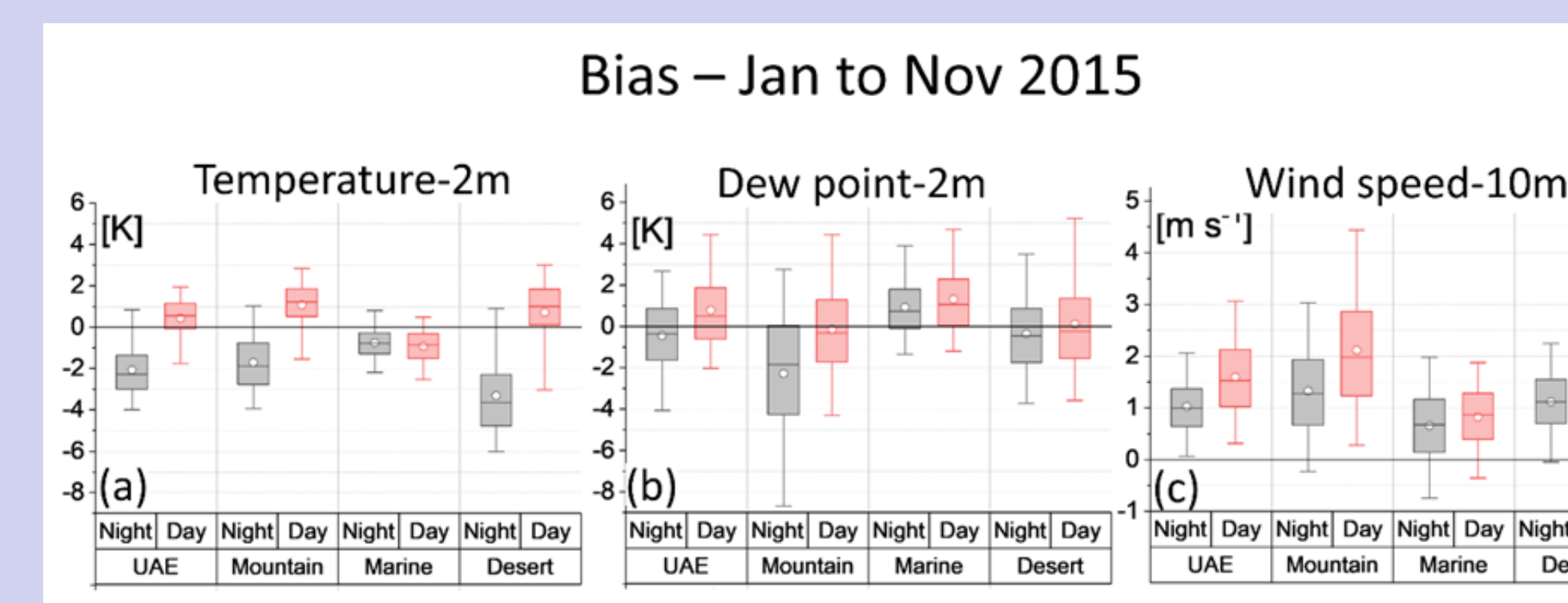
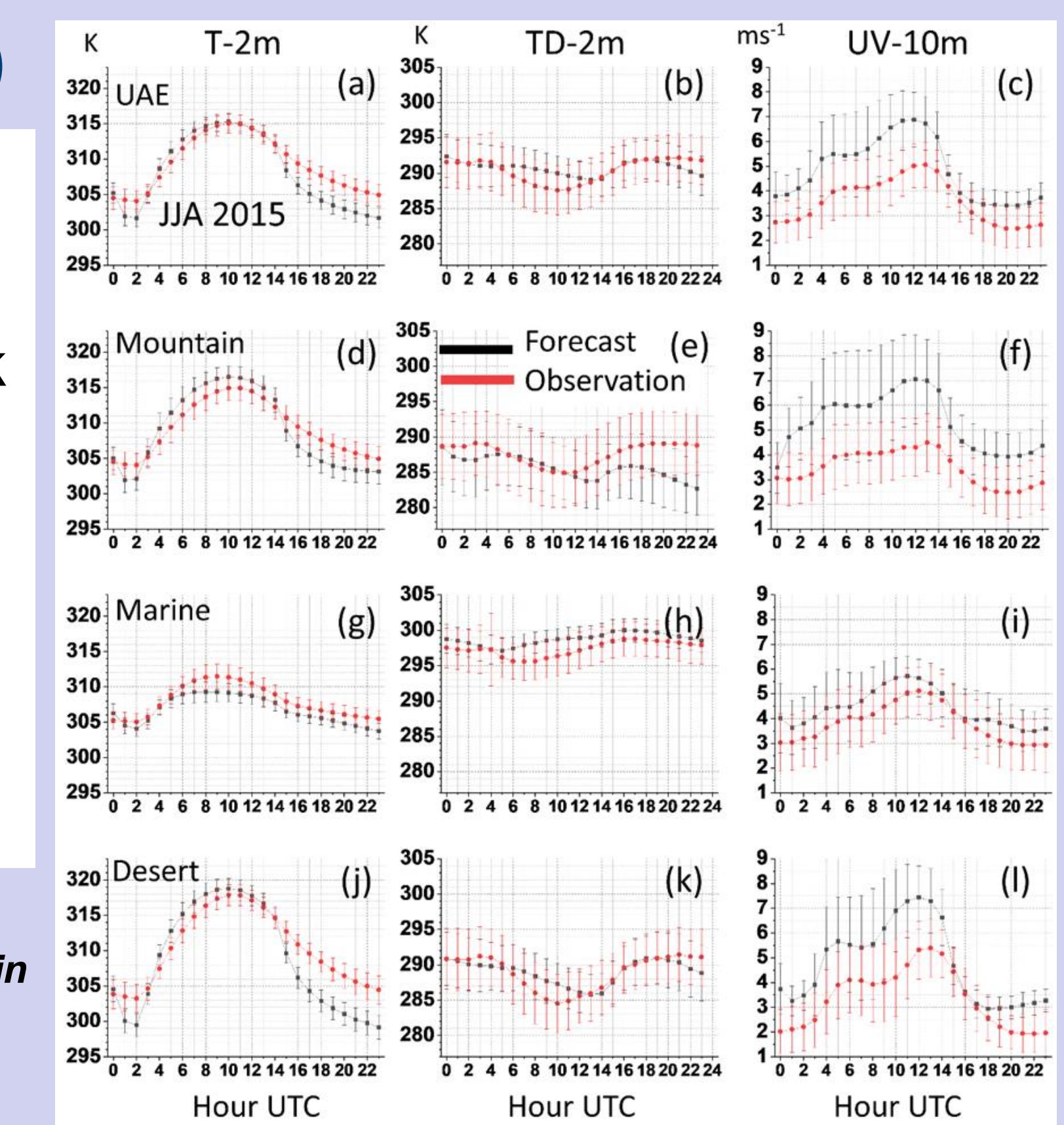


Figure 5: Box plots of bias for 2m air temperature, dew point and 10 m windspeed - panels (a-c) respectively for all time steps over the period of Jan-Nov 2015. Statistics are divided by region (UAE, Mountain, Marine, Desert) and then by nighttime and daytime hours (respectively, nighttime 18:00-05:00 (grey boxes) and daytime 06:00-17:00 (red boxes) in local time). On the box plots the centre line represents the mean, the white circle is the median, box ends are 25% and 75% percentiles and the whiskers are 5% and 95 % percentiles. Also marked is a zero-reference line.

The aim of this study was to assess the skill of the model in reproducing surface quantities over the UAE.

- Temperature biases are usually below 1 K during daytime, but larger during night (especially in the desert).
- Dewpoint is relatively well represented with biases generally smaller than 1 K.
- Wind speeds are generally over-estimated in WRF, especially during day with biases up to 2 m/s.

Figure 6: Diurnal cycles of mean summer (JJA) WRF forecasts (black) compared to observations (red) within different regions. In each plot the mean and standard deviation is shown. Variables are temperature, dew point, and windspeed.



4) Air quality forecast system for Stuttgart

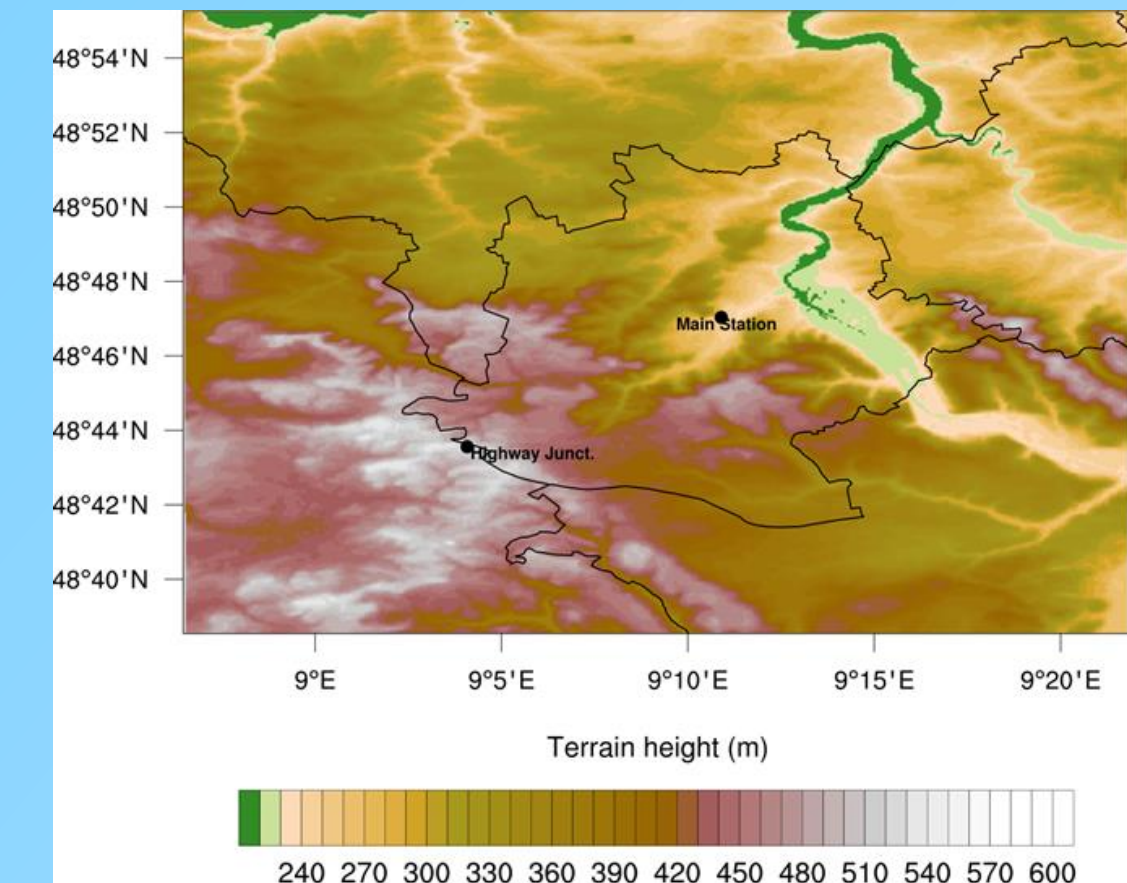


Figure 7: Innermost model domain with 50 m horizontal resolution.

- WRF version 4.0.3 including chemistry module was set up in a three domain configuration with 1250 m, 250 m and 50 m resolution and 100 vertical levels up to 50 hPa.
- Domain sizes of 800 x 800, 601 x 601 and 601 x 601 grid cells.
- Sophisticated initialization of topography, land cover and soil characteristics from high-resolution data.
- Initialization of chemical emissions from different sources with resolutions down to 500 m.



Figure 9: Simulated NO₂ concentrations (µg/m³) during the morning peak traffic time on January 21, 2019. The viewing direction is from northeast to southwest with the Stuttgart main station in the foreground. Brownish colors indicate high concentrations (Image courtesy: Leyla Kern, HLRs).

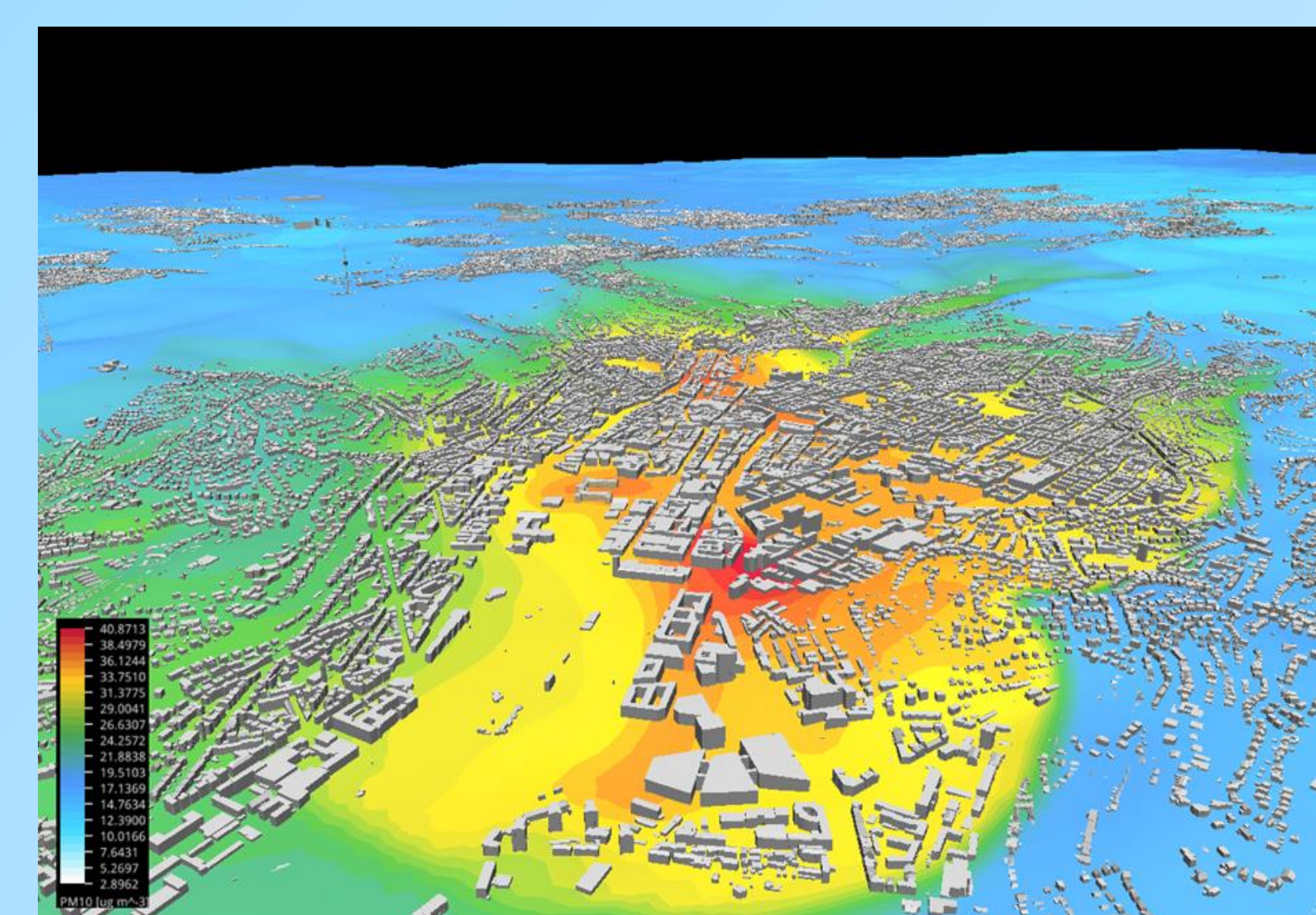


Figure 10: Same as Figure 9 but for PM10. Red colors denote high PM10 concentrations. (Image courtesy: Leyla Kern, HLRs).

- The near-surface circulation along the Neckar valley and upslope flows after sunrise are well represented by the model.
- Realistic simulation of higher concentrations along the main roads and downtown in the city center region.
- Morning and evening rush hour episodes are well represented.
- During day, developing turbulence mixes up the pollutants in the boundary layer and largely reduces the near surface values.
- High concentrations only appear in the lowest model levels.

5) Assimilation of lidar water vapor measurements

- Water vapor lidar data from a 10-hour episode was assimilated in a rapid update cycle (RUC) with hourly analyses.
- WRF was setup with one domain, 2.5 km horizontal resolution and 100 vertical levels up to 50 hPa.
- With 3DVAR and hybrid 3DVAR-ETKF, the performances of two different assimilation methods were investigated.

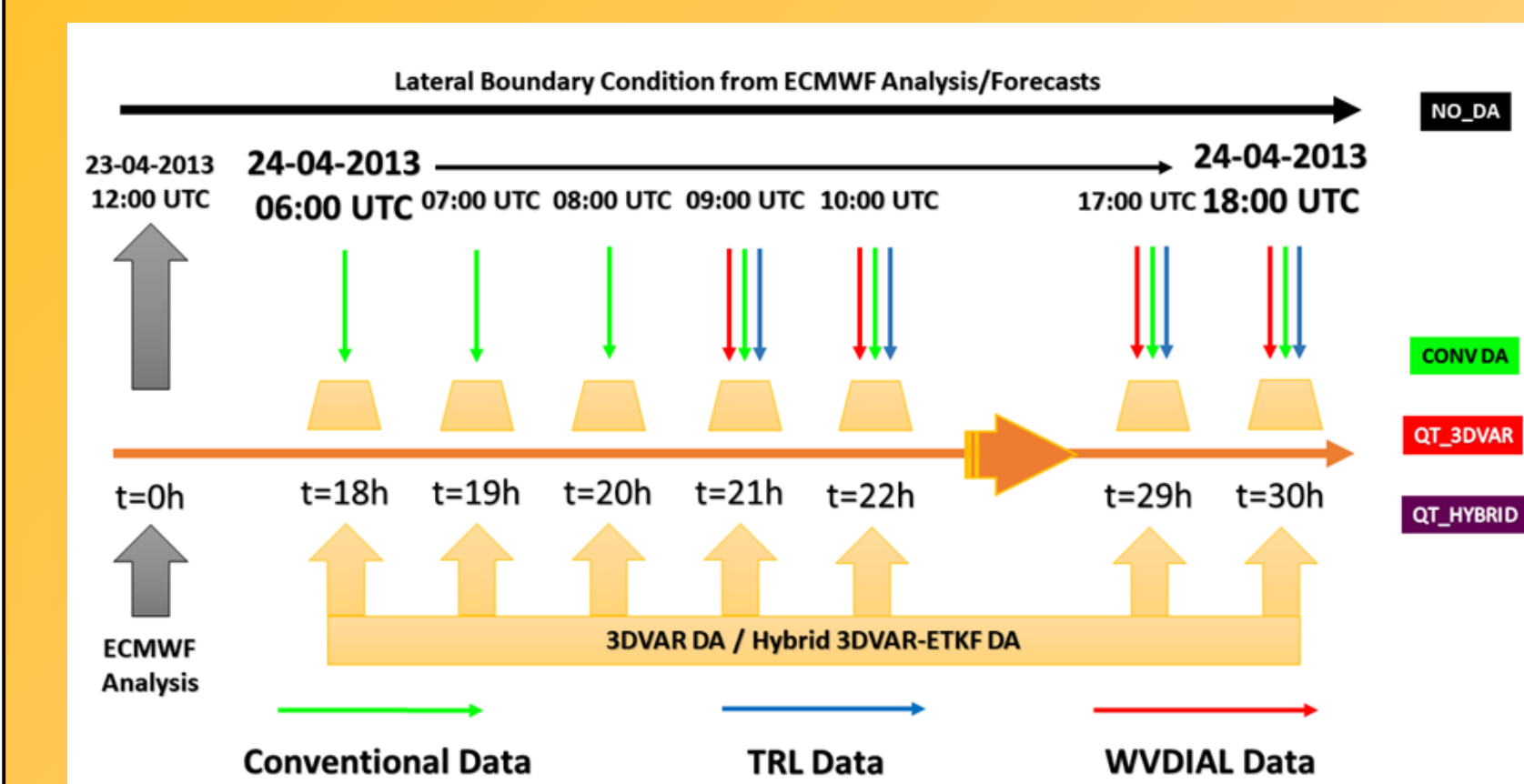


Figure 11: Temporal setup of the assimilation experiments.

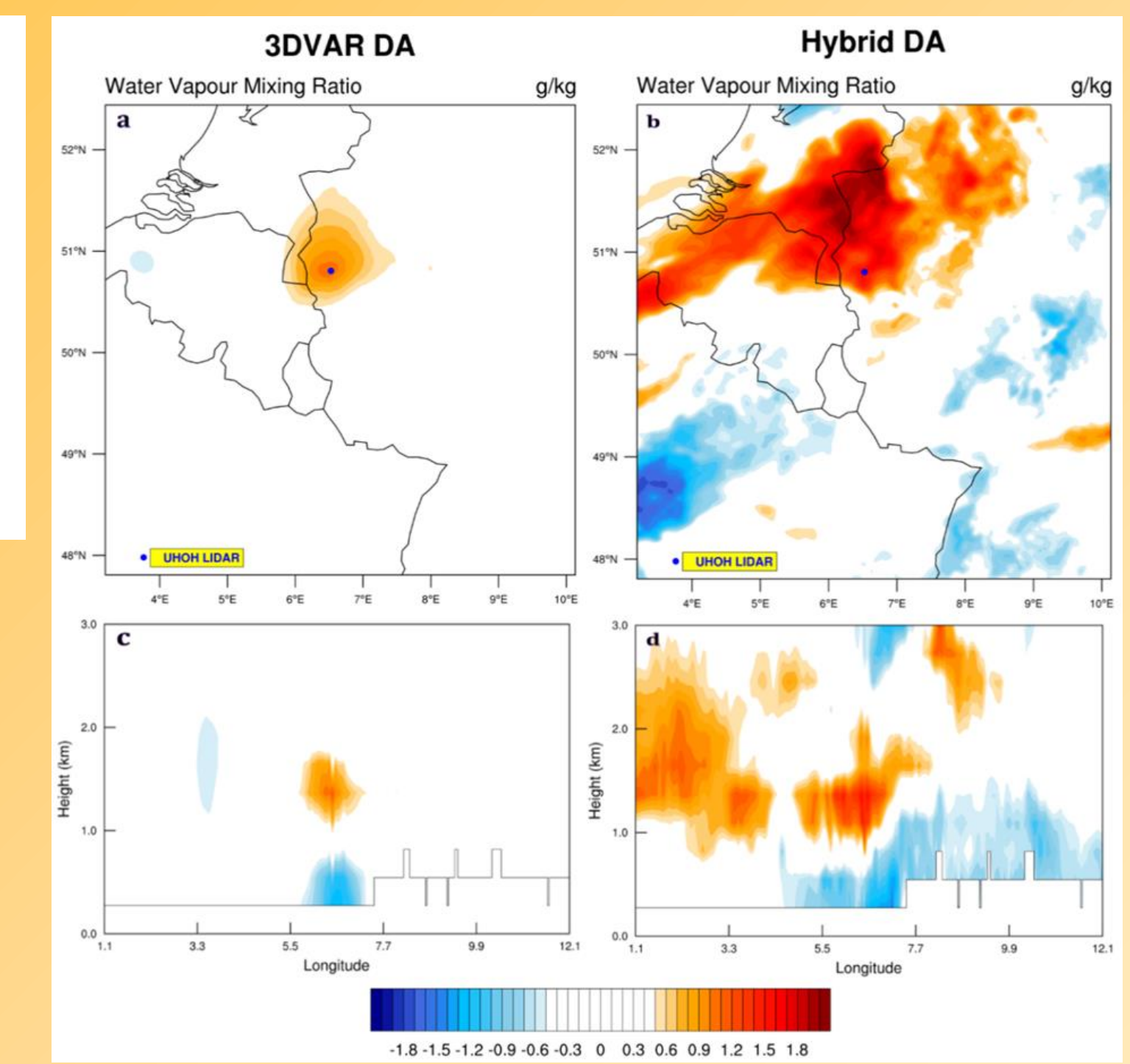


Figure 12: a) Water vapor mixing ratio analysis increment after 10 3DVAR DA cycles. b) Same but after 10 Hybrid DA cycles. a and b are spatial plots at 1200 m above ground level, and, c and d are vertical cross-sections.

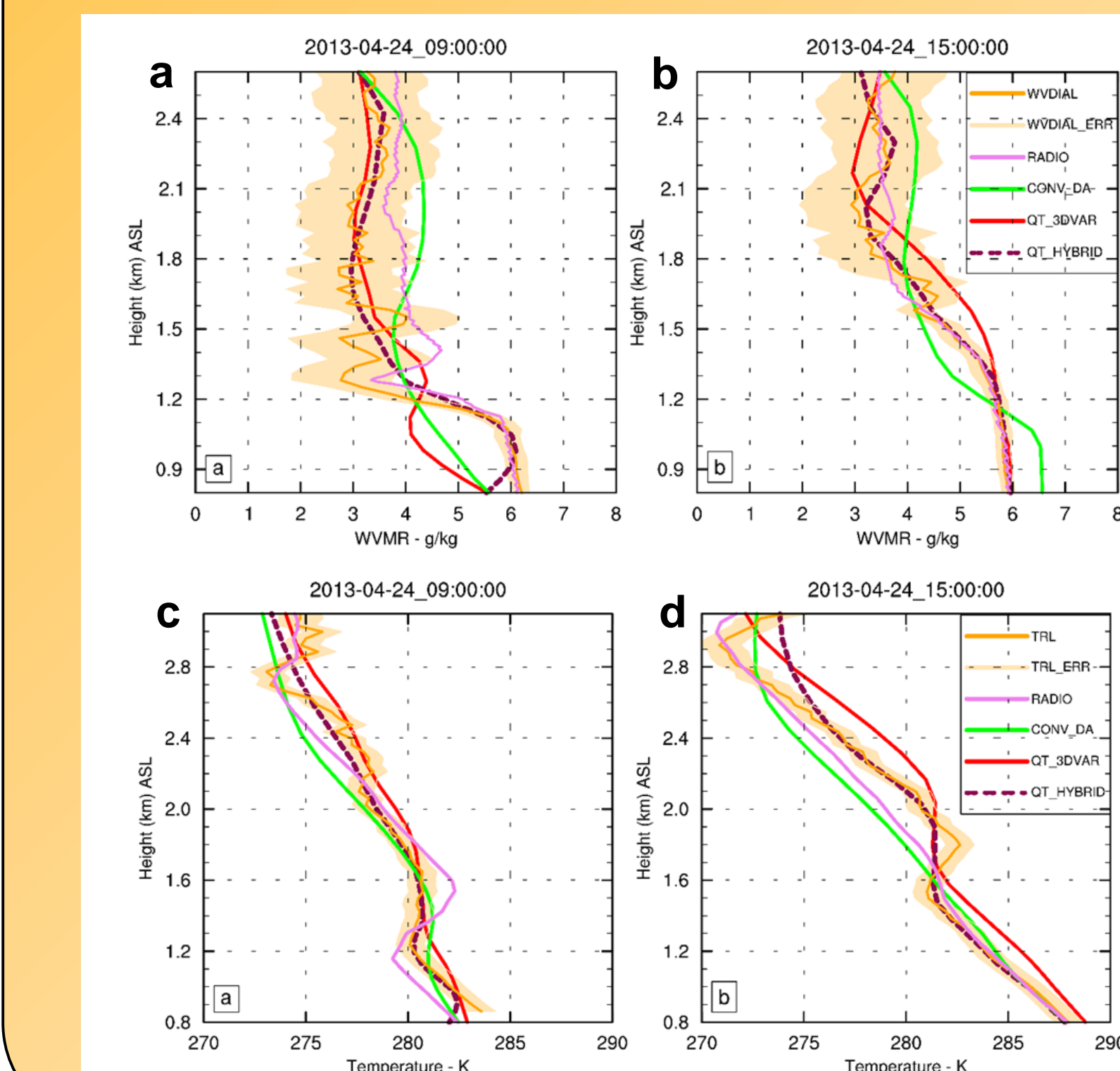


Figure 13: a) Water vapor mixing ratio profile during the first assimilation. b) Same profile at 15 UTC after 6 assimilation cycles. c) Temperature profile during the first assimilation. d) Same profile at 15 UTC after 6 assimilation cycles.

- The assimilation of lidar water vapor data improves the forecast performance of the model with both methods.
- The propagation of the background error covariance matrix in the hybrid method influences a clearly larger region and has an additional beneficial impact on the forecast performance compared to 3DVAR.
- Disagreement of forecast and observation between 1.5 and 2 km above sea level is caused by the coarse vertical resolution of the simulations.

Bauer, H.-S., S. K. Muppa, V. Wulfmeyer, A. Behrendt, K. Warrach-Sagi, and F. Späth, 2020: Multi-nested WRF simulations for studying planetary boundary layer processes on the turbulence-permitting scale in a realistic mesoscale environment. *Tellus A: Dynamic Meteorology and Oceanography*, 72(1), 1-28

Branch, O., V. Wulfmeyer, 2019: Deliberate enhancement of rainfall using desert plantations. *Proc. Natl. Acad. Sci. U.S.A.* 116, 18841-18847.

Schwitalla, T., H.-S. Bauer, K. Warrach-Sagi, T. Boenisch and V. Wulfmeyer, 2020: Turbulence-permitting air pollution simulation for the Stuttgart metropolitan area, *Atmos. Chem. Phys.*, submitted.

Thundathil, R., T. Schwitalla, A. Behrendt, S. K. Muppa, S. Adam, and V. Wulfmeyer, 2020: Assimilation of lidar water vapour mixing ratio and temperature profiles into a convection-permitting model. *J. Meteor. Soc. Japan* 98, 5.